ACS APPLIED ENERGY MATERIALS

Letter

Cite This: ACS Appl. Energy Mater. 2018, 1, 6714−6718

www.acsaem.org

Differential Electrochemical Mass Spectrometry of Carbon Felt Electrodes for Vanadium Redox Flow Batteries

L. Eifert,[†] Z. Jusys,[‡] R. Banerjee,[†] R. J. Behm,[‡] and R. Zeis*[,†,§]

[†]Karlsruhe Institute of Technology, Helmholtz Institute Ulm, Helmholtzstraße 11, D-89081 Ulm, Germany

[‡]Institute of Surface Chemistry and Catalysis, Ulm University, Albert-Einstein-Allee 47 D-89081 Ulm, Germany

[§]Institute of Physical Chemistry, Karlsruhe Institute of Technology, Fritz-Haber-Weg 2, D-76131 Karlsruhe, Germany

Supporting Information

ABSTRACT: We successfully conducted electrochemical and online mass spectrometric measurements on commercial carbon felt electrodes with a differential electrochemical spectrometry setup. Its capability is demonstrated by simultaneous mass spectrometric and electrochemical measurements. Half-cell tests, such as cyclic voltammetry, and coulometry of the redox couples can be performed under stopped flow of the electrolyte. We use different potential windows, and two types of electrolytes while monitoring potential dependent H_2, O_2 and CO_2 formation. At oxidizing potentials, we did not observe oxygen evolution, only carbon corrosion. An increase in CO_2 and H_2 formation at high and low potentials in the presence of vanadium is observed.

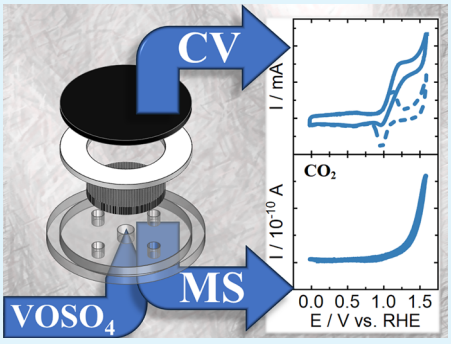

KEYWORDS: *vanadium redox flow battery, differential electrochemical mass spectrometry, DEMS, carbon felt, carbon corrosion*

Carbon fibers in the form of paper or felts are the most common electrode material for vanadium redox flow batteries (VRFBs). Their physical and chemical properties strongly influence the overall cell performance, and their degradation due to unwanted side reactions (carbon corrosion and oxygen and hydrogen evolution) is partially responsible for the performance losses.[1,2]

Differential electrochemical spectrometry (DEMS) has been proven to be suitable characterizing carbon materials, mainly in the context of fuel cell research.[3−5] Recently, Taylor et al. used DEMS to calculate the faradaic efficiency of the V^{3+} reduction reaction on the oxidized edge and basal surfaces of graphite discs in a model study on the activity and stability of the negative electrode in VRFBs.[6]

Although DEMS is a straightforward technique to investigate volatile components under potential control, it has not yet been applied to study the corrosion of carbon felts under reaction conditions, namely, in the presence of vanadium ions and under continuous electrolyte flow. The latter issue is one of the major obstacles for the long-term durability of carbon felt electrodes, which are commonly used in the vanadium redox flow batteries. In this study we present a modification of a DEMS flow cell,[7] which enables mounting of the commercial carbon felts as a working electrode for conducting simultaneous electrochemical and online mass spectrometric experiments. Furthermore, we will demonstrate that the vanadium redox processes in the confined volume within the carbon felt can be quantitatively assessed under the stopped electrolyte flow, though the mass spectrometric detection of gaseous products is no more possible under these conditions.

Shortly, the DEMS setup[8] consists of a modified version of the previously introduced dual thin-layer flow-through cell.[7] By employing a PTFE spacer, a cylindrical cut-out of the carbon felt can be mounted in it. The carbon felts used in this study are thermally treated as described previously in the literature.[1,9,10] The felts were first measured in sulfuric acid, followed by the vanadium containing electrolyte. Each time the felts were cycled until a stable voltammogram was achieved and thus all volatile components in the felt were removed. More experimental details are provided in the Supporting Information.

The influence of the electrolyte composition on carbon corrosion was investigated in an oxidative potential range. Figure 1 shows the potential dependent CO_2 formation (a), as well as the corresponding cyclic voltammograms (b) in sulfuric acid supporting electrolyte (red) and in the vanadium electrolyte (blue) under conditions of continuous electrolyte flow (solid lines), as well as without electrolyte flow (dashed lines).

The CO_2 formation in vanadium containing electrolyte during the positive-going scan onset at ca. 0.9 V (see inset of Figure 1a) together with the onset of V^{4+} oxidation to V^{5+} (see inset of Figure 1b), indicating ca. 0.3 V earlier oxidation of carbon felt in the vanadium containing electrolyte compared to supporting electrolyte. With the further progress of electrode potential, the CO_2 formation remains faster in comparison,

Received: September 13, 2018
Accepted: November 13, 2018
Published: November 13, 2018

DOI: 10.1021/acsaem.8b01550
ACS Appl. Energy Mater. 2018, 1, 6714−6718

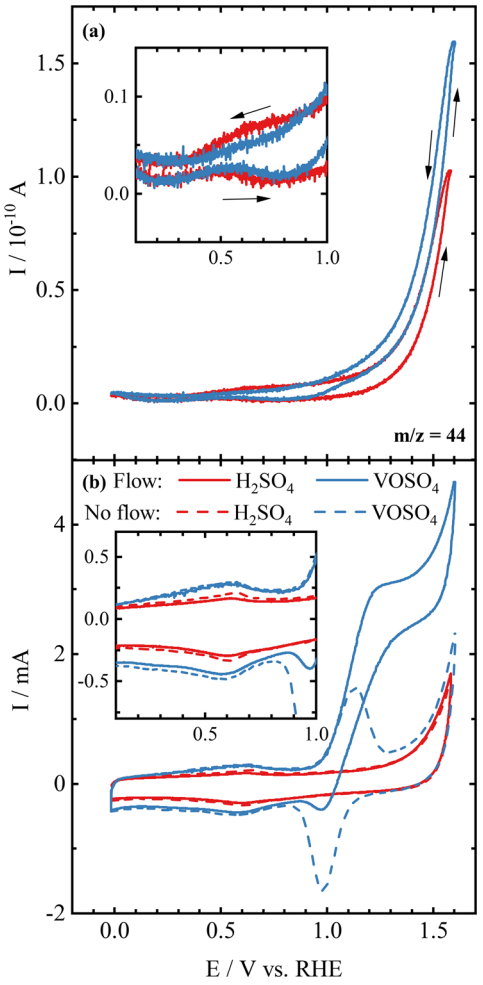

Figure 1. MS signals of CO_2 (a) and the cyclic voltammograms (b) in the oxidative range. The insets show a close-up of the quinone/hydroquinone redox peak region. The potential scan was 10 mV/s; the electrolyte (5 mM $VOSO_4$ in 2 M H_2SO_4) flow rate was about 6 μL/s.

approaching an about one-third higher rate at the positive potential limit applied. This clearly coincides with oxidation of V^{4+} to V^{5+}, as confirmed by the mass transport limited current for vanadium oxidation of around 3 mA, which is reached at 1250 mV (Figure 1b). This is followed by a current increase due to carbon corrosion at higher potentials, as evidenced from the CO_2 formation. Comparing the increase of the faradaic current from ca. 1.3 to 1.6 V, they are approximately the same in both, vanadium containing and supporting electrolyte, although in the latter, the CO_2 formation is significantly higher, which could be tentatively attributed to V^{5+} (VO_2^+) promoted oxidation of carbon.

During the reverse sweep, a current plateau of around 2 mA is reached, with the mass transport current superimposed by a broad capacitive feature of the carbon felt electrode. This is followed by a small reduction peak of −0.4 mA at 990 mV, which can be attributed to the reduction of V^{5+} residue that remained inside the felt, as confirmed by the measurement at stopped flow (dashed blue line). A higher flow rate or slower potential scan rate might reduce this effect.

During the oxidation of hydroquinone to quinone at 500 mV, a low rate of CO_2 formation can be observed in both electrolytes. However, there is no vanadium redox activity in this potential range, as expected and evidenced by both flow and stopped flow measurements.

Under the stopped flow conditions, two distinct redox peaks in the vanadium containing electrolyte can be observed. This corresponds to the V^{4+}/V^{5+} redox with peak potentials of ca. 1.13 and 0.98 V for anodic and cathodic peaks (peak separation ΔE = 147 mV), respectively, a anodic to cathodic peak current ratio (I_A/I_C) of 0.86, and a charge ratio (C_A/C_C) of 1.03 (see Table 1). In the confined volume within the carbon felt electrode, this indicates a high reversibility of the redox reaction. Finally, for the sulfuric acid supporting electrolyte, stopping the electrolyte flow did not alter the cyclic voltammogram, since all the features depend only on the electrode surface, which suffers from the electrochemical oxidation at potentials more positive than ca. 1.3 V at a similar amount as that under the electrolyte flow.

Table 1. Electrochemical Data of the V^{4+}/V^{5+} (A1, Anodic; C1, Cathodic) and V^{2+}/V^{3+} (A2, Anodic; C2, Cathodic) Redox Reactions in the Oxidative (ox.; 0.0−1.6 V), Full (−0.4−1.6 V), and Reductive (red.; −0.4−0.0 V) Potential Range without Flow[a]

range	peak	E (V)	I (mA)	C (mC)	ΔE (mV)	I_A/I_C	C_A/C_C
ox.	A1	1.128	1.26	23.59	147	0.86	1.03
ox.	C1	0.981	−1.47	−22.83			
full	A1	1.153	3.11	42.03	163	2.16	1.96
full	C1	0.990	−1.44	−21.54			
full	A2	−0.286	1.01	8.46			0.30
full	C2			−28.12			
red.	A2	−0.293	1.58	18.48	57	0.93	0.94
red.	C2	−0.350	−1.70	−19.62			

[a] E, potential; I, current; C, charge.

Figure 2 shows the potential dependent (a) CO_2, (b) H_2 and (c) O_2 formation, as well as the corresponding cyclic voltammogram (d) in sulfuric acid (red) and in the vanadium electrolyte (blue) in the potential range extended to the hydrogen evolution under continuous flow of electrolyte. The dashed voltammograms in Figure 2d represent the measurements without the electrolyte flow.

After scanning the electrode potential to −0.4 V in the vanadium-free supporting electrolyte, in the positive-going scan an earlier onset and larger amounts of CO_2 formation can be observed around the hydroquinone oxidation at approximately 400 mV, compared to the measurement with the lower potential limit of 0.0 V (Figure 1a). At higher potentials, the CO_2 formation increases exponentially, starting from ca. 1200 mV (see Figure 2a and its inset). Both indicate that the reduced carbon surface at lower potentials is more easily oxidized, and at the positive potentials, where the CO_2 formation rate is ca. 30% higher compared to the measurement using the low potential limit not exceeding 0.0 V. In the vanadium containing electrolyte, CO_2 formation sets in at around 100 mV, reaches a plateau, followed by the second increase with the onset of the V^{4+} oxidation and then increases exponentially positive of 1200 mV, exhibiting a rather similar CO_2 formation rate at the upper potential limit as that in the sulfuric acid solution. The differences between the onset potentials of CO_2 formation can be explained by the oxidative nature of V^{5+} (which is present in the form of VO_2^+), as

DOI: 10.1021/acsaem.8b01550
ACS Appl. Energy Mater. 2018, 1, 6714−6718

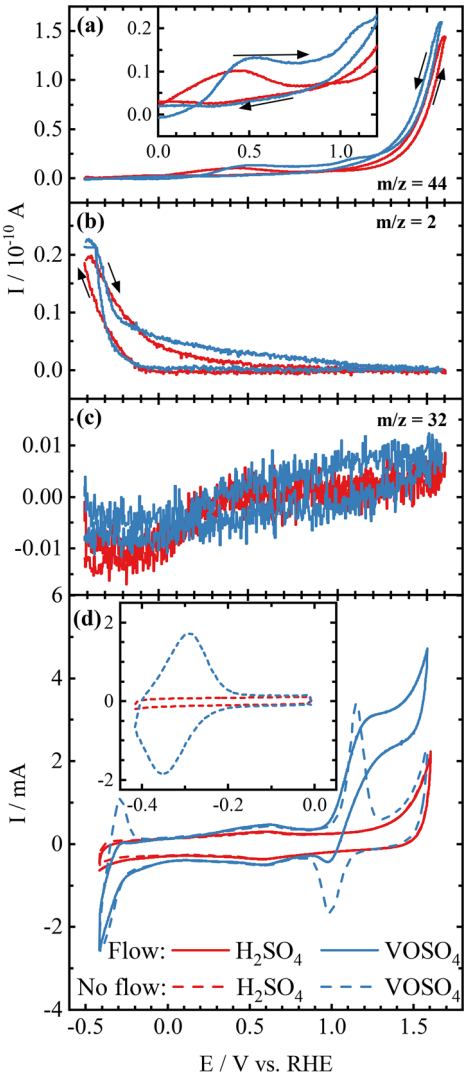

Figure 2. Potential dependent (a) CO_2, (b) H_2, and (c) O_2 formation, as well as the corresponding cyclic voltammogram (d) in sulfuric acid (red) and the vanadium electrolyte (blue). The dashed voltammograms represent the measurement without electrolyte flow. The potential scan was 10 mV/s; the electrolyte (5 mM $VOSO_4$ in 2 M H_2SO_4) flow rate was about 6 μL/s. The inset in panel d shows a stable cyclic voltammogram of the V^{2+}/V^{3+} redox couple in the low potential range at a stopped flow.

discussed previously. However, at low potential, reduced carbon is facile for electrochemical oxidation as it could be seen from nearly equal CO_2 formation rates at the positive potential limit.

For the hydrogen evolution (Figure 2c), we observe an influence of the respective vanadium species similar to that for the carbon corrosion: The reduction of V^{4+} to V^{2+} ions (see Table 1 and related further discussion) leads to a more pronounced hydrogen formation, which implies that some water gets reduced by the oxidation of V^{2+}. This confirms the observation by Sun et al.,[13] who stated that V^{2+} electrolytes form H_2 in the presence of carbon felts under open circuit conditions, which implies the formation of a mixed potential.[14,15] However, this is in contrast to the findings reported by Taylor et al.,[6] where the suppression of hydrogen evolution in the presence of ca. 1.5 M of V^{3+} was found, which could be related to much higher vanadium concentration and the different carbon electrode materials. In addition, in our experiments V^{4+} rather than V^{3+} solution was used.

The electrochemical current at low potentials in the V^{4+} containing electrolyte under continuous electrolyte flow is much higher, compared to the supporting electrolyte under the same conditions, which indicates the reduction of V^{4+} to a lower oxidation state, since no V^{4+} reduction current is observed in the potential range from 0.9 to 0.1 V. It must be noted here that the mass transport limited current for the low potential reduction of V^{4+} cannot be reached going to even lower potential due the exponential increase of hydrogen evolution.[5,11] Otherwise, the height of mass transport limited current could simply indicate how many electrons are transferred in the reduction of V^{4+}: for one electron reduction to V^{3+} the absolute current should be equal to the mass transport limited current for V^{4+} oxidation to V^{5+}, whereas for two-electron reduction of V^{4+} to V^{2+} the current should be twice as high. The mass transport limited current of the oxidation of V^{4+} to V^{5+} is similar to that obtained in the oxidative potential (Figure 1b), which indicates that it is not significantly affected by the lower potential limit applied.

In addition, the lower solubility of gaseous hydrogen compared to carbon dioxide results in bubble formation, which in some cases can disturb the MS data, as it is visible in Figure 2b in the vanadium containing electrolyte.

Interestingly, we do not observe any significant oxygen evolution at high potentials (Figure 2c), which contradicts earlier presumptions in the literature.[11,12] At low potentials, some consumption of oxygen can be attributed to the reduction of trace amounts delivered by the flowing electrolyte.

Due to the lack of the mass transport current for the reduction of V^{4+} under continuous flow of electrolyte because of the interference with H_2 evolution, the electrochemical measurements were performed under the stopped flow conditions. Here, the trapped constant amount of vanadium ions in the confined space within the carbon felt can be sequentially reduced or oxidized at the defined potentials, allowing for the coulometric analysis of corresponding redox pairs. The dashed blue line in Figure 2d depicts the cyclic voltammetry profile of a carbon felt electrode in V^{4+} containing electrolyte under stopped flow conditions in a wide potential range from −0.4 to 1.6 V. The reduction current reached at the lower potential limit is similar to that under continuous flow (solid blue line, Figure 2d), but in the backward scan an oxidation peak at ca. −0.3 V appears under the stopped flow conditions.

Going further positive, after passing a small hydroquinone oxidation peak at ca. 0.6 V, which is slightly higher for the reduced carbon felt, an expressed oxidation peak appears at ca. 1.15 V under the stopped flow conditions. Its peak current is significantly higher compared to the V^{4+} oxidation to V^{5+} when applying the low potential limit of 0.0 V (Figure 1b), whereas the reduction peak of V^{5+} to V^{4+} is similar, irrespective of the lower potential limit, which would be expected for the same amount of vanadium trapped in the confined space. However, the difference of the oxidation peak depending on the lower limit could be explained by considering that not only V^{4+} is oxidized but also the lower oxidation state ions, formed upon the reduction of V^{4+} at low potentials. If V^{4+} is at low potentials reduced to V^{3+}, it is reoxidized to V^{4+} at −0.3 V, and thus this would not lead to an increased oxidation current to V^{5+}, in contrast to results of Figure 1b and Figure 2d. For the case of reduction of V^{4+} to V^{2+} at low potentials, the latter will be

DOI: 10.1021/acsaem.8b01550
ACS Appl. Energy Mater. 2018, 1, 6714−6718

oxidized to V^{3+} at −0.3 V, still residing in the carbon felt under the stopped flow conditions, until V^{3+} will be oxidized together with V^{4+} to V^{5+}, which would result in about double current, compared to only V^{4+} oxidation to V^{5+}.[15]

To support this hypothesis, the results of quantitative evaluation of the electrochemical data are listed in Table 1. In the oxidative (ox.; plot shown in Figure 1b, dashed line) potential region the oxidation and reduction charge is nearly identical for the V^{4+}/V^{5+} redox couple. In the wide (full; plot shown in Figure 2d, dashed line) potential window, however, the oxidation charge for the peak at ca. 1.15 V is about twice higher than the V^{5+} reduction charge, the latter being identical to that in the oxidative potential region. This clearly indicates a two-electron transfer in oxidation reaction to V^{5+}, after the excursion to −0.4 V, where V^{4+} is reduced to V^{2+} during the negative-going scan and reoxidized to V^{3+} in the backward scan, which is further oxidized to V^{5+} at higher potentials. However, since the reduction of V^{4+} to V^{2+} at a low potential is overlapping with hydrogen evolution, the charge for oxidation of V^{2+} to V^{3+} is ca. 3-fold lower than that for the cumulative reduction. To isolate the V^{2+} to V^{3+} redox couple for avoiding further oxidation to V^{5+}, the upper potential limit was set to 0.0 V. As a consequence, the reduction current was gradually decreasing, and the oxidation counterpart correspondingly increasing, finally resulting in a stable voltammetric redox pair (inset in Figure 2d) resulting in an equal charge for the reduction and oxidation reactions, which is close to the charge of V^{4+}/V^{5+} redox pair in the oxidative region. Based on the redox processes being around −0.30 and −0.35 V under these conditions they can be assigned to a reversible V^{2+}/V^{3+} redox pair developed in the confined space at a stopped flow.

In this study, we were able to successfully conduct electrochemical and online mass spectrometric measurements on commercially available carbon felt electrodes with a DEMS setup under continuous electrolyte flow conditions. At oxidative potentials a mass transport limited current for V^{4+} oxidation V^{5+} is reached under continuous flow of electrolyte, followed by the increase of current due to carbon oxidation to CO_2, whereas no oxygen evolution can be detected. By comparing the electrochemical behavior in sulfuric acid base electrolyte and in vanadium containing electrolyte, we demonstrated that the presence of vanadium ions has a profound effect, leading to 50% higher CO_2 formation and a lower onset potential in the oxidative potential regions. This implies that the previously oxidized V^{5+} acts as an oxidizing agent versus the carbon electrode. A small reduction peak during the anodic scan during flowing vanadium electrolyte indicates the presence of residual V^{5+} inside the felt, which could be reduced by a higher flow rate. The increased H_2 formation in the presence of V^{2+} ions suggests that some water gets also reduced by the oxidation of V^{2+}. In addition, the electrochemical half-cell tests, such as cyclic voltammetry and coulometry of the redox couples, can be performed under stopped flow of the electrolyte, where the respective vanadium redox pairs demonstrate a reversible behavior for the electrolyte trapped in the confined volume in the carbon felt electrode.

Further investigations with DEMS using different felt types can enable a more extensive understanding of the degradation mechanisms of the felt and therefore aid the development of improved materials for the VRFB.

■ ASSOCIATED CONTENT

Supporting Information

The Supporting Information is available free of charge on the ACS Publications website at DOI: 10.1021/acsaem.8b01550.

Carbon materials, experimental setup, and experimental procedure and techniques (PDF)

■ AUTHOR INFORMATION

Corresponding Author

*Tel.: +49 (731) 50 34700. E-mail: roswitha.zeis@kit.edu.

ORCID

R. J. Behm: 0000-0002-7565-0628

R. Zeis: 0000-0001-8379-0578

Notes

The authors declare no competing financial interest.

■ ACKNOWLEDGMENTS

We gratefully acknowledge financial support by the German Federal Ministry of Education and Research (BMBF) in Project 03X4636C and the Impuls- and Vernetzungsfonds der Helmholtz Gesellschaft (Young Investigator Group Project VH-NG-616). We gratefully acknowledge SGL Carbon for the supply of SIGRACELL carbon felts. This work contributes to the research performed at CELEST (Center for Electrochemical Energy Storage Ulm-Karlsruhe).

■ REFERENCES

(1) Eifert, L.; Banerjee, R.; Jusys, Z.; Zeis, R. Characterization of Carbon Felt Electrodes for Vanadium Redox Flow Batteries: Impact of Treatment Methods. *J. Electrochem. Soc.* **2018**, *165*, A2577−A2586.

(2) Banerjee, R.; Bevilacqua, N.; Eifert, L.; Zeis, R. Characterization of Carbon Felt Electrodes for Vanadium Redox Flow Batteries − A Pore Network Modeling Approach. *J. Energy Storage* **2018**, manuscript accepted.

(3) Colmenares, L. C.; Wurth, A.; Jusys, Z.; Behm, R. J. Model Study on the Stability of Carbon Support Materials under Polymer Electrolyte Fuel Cell Cathode Operation Conditions. *J. Power Sources* **2009**, *190*, 14−24.

(4) Ashton, S. J.; Arenz, M. Comparative DEMS Study on the Electrochemical Oxidation of Carbon Blacks. *J. Power Sources* **2012**, *217*, 392−399.

(5) Pérez-Rodríguez, S.; Sebastián, D.; Lázaro, M. J.; Pastor, E. Stability and Catalytic Properties of Nanostructured Carbons in Electrochemical Environments. *J. Catal.* **2017**, *355*, 156−166.

(6) Taylor, S. M.; Pătru, A.; Perego, D.; Fabbri, E.; Schmidt, T. J. Influence of Carbon Material Properties on Activity and Stability of the Negative Electrode in Vanadium Redox Flow Batteries: A Model Electrode Study. *ACS Appl. Energy Mater.* **2018**, *1*, 1166−1174.

(7) Jusys, Z.; Massong, H.; Baltruschat, H. A New Approach for Simultaneous DEMS and EQCM: Electro-oxidation of Adsorbed CO on Pt and Pt-Ru. *J. Electrochem. Soc.* **1999**, *146*, 1093−1098.

(8) Heinen, M.; Chen, Y. X.; Jusys, Z.; Behm, R. J. In Situ ATR-FTIRS Coupled with on-Line DEMS under Controlled Mass Transport Conditions-A Novel Tool for Electrocatalytic Reaction Studies. *Electrochim. Acta* **2007**, *52*, 5634−5643.

(9) Pezeshki, A. M.; Clement, J. T.; Veith, G. M.; Zawodzinski, T. A.; Mench, M. M. High Performance Electrodes in Vanadium Redox Flow Batteries through Oxygen-Enriched Thermal Activation. *J. Power Sources* **2015**, *294*, 333−338.

(10) Sun, B.; Skyllas-Kazacos, M. Modification of Graphite Electrode Materials for Vanadium Redox Flow Battery Application—I. Thermal Treatment. *Electrochim. Acta* **1992**, *37*, 1253−1260.

(11) Schnucklake, M.; Kuecken, S.; Fetyan, A. M.; Schmidt, J.; Thomas, A.; Roth, C. Salt-Templated Porous Carbon-Carbon

DOI: 10.1021/acsaem.8b01550
ACS Appl. Energy Mater. 2018, 1, 6714−6718

Composite Electrodes for Application in Vanadium Redox Flow Batteries. *J. Mater. Chem. A* **2017**, *5*, 25193−25199.
(12) Wei, L.; Zhao, T. S.; Xu, Q.; Zhou, X. L.; Zhang, Z. H. In-Situ Investigation of Hydrogen Evolution Behavior in Vanadium Redox Flow Batteries. *Appl. Energy* **2017**, *190*, 1112−1118.
(13) Sun, C. N.; Delnick, F. M.; Baggetto, L.; Veith, G. M.; Zawodzinski, T. A. Hydrogen Evolution at the Negative Electrode of the All-Vanadium Redox Flow Batteries. *J. Power Sources* **2014**, *248*, 560−564.
(14) Spiro, M. Polyelectrodes: The Behaviour and Applications of Mixed Redox Systems. *Chem. Soc. Rev.* **1986**, *15*, 141−165.
(15) Liu, M.; Xiang, Z.; Deng, H.; Wan, K.; Liu, Q.; Piao, J.; Zheng, Y.; Liang, Z. Electrochemical Behavior of Vanadium Redox Couples on Carbon Electrode. *J. Electrochem. Soc.* **2016**, *163*, H937−H942.

DOI: 10.1021/acsaem.8b01550
ACS Appl. Energy Mater. 2018, 1, 6714−6718